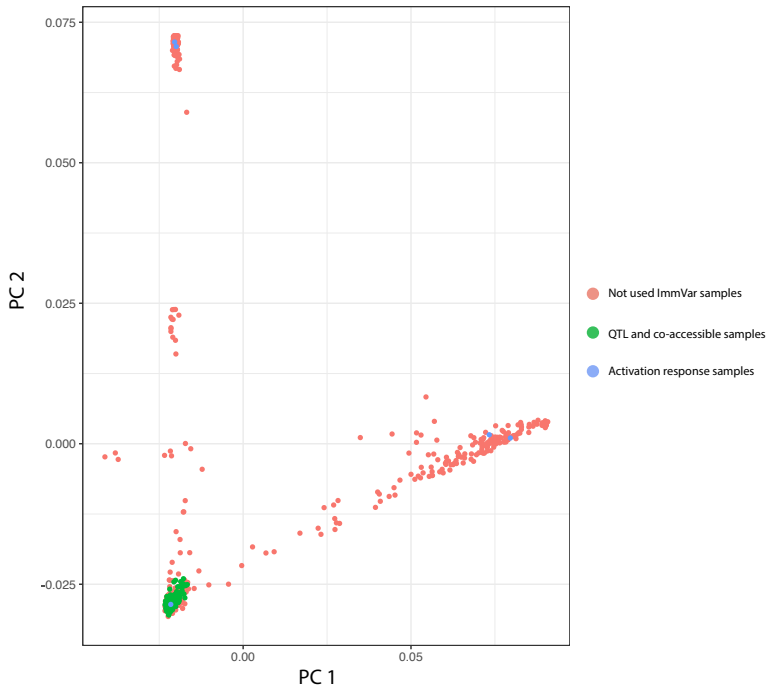

Supplementary Figure 1. PCA of the genetic relationships between individuals in the ImmVar cohort. Shown are the scores for each of 688 individuals in the ImmVar Consortium along the first two principal components (PCs, x and y-axes) in a PCA of the genetic relationship matrix. Individuals used in this study are highlighted in blue (activation response analysis) and green (QTL and co-accessibility analyses).

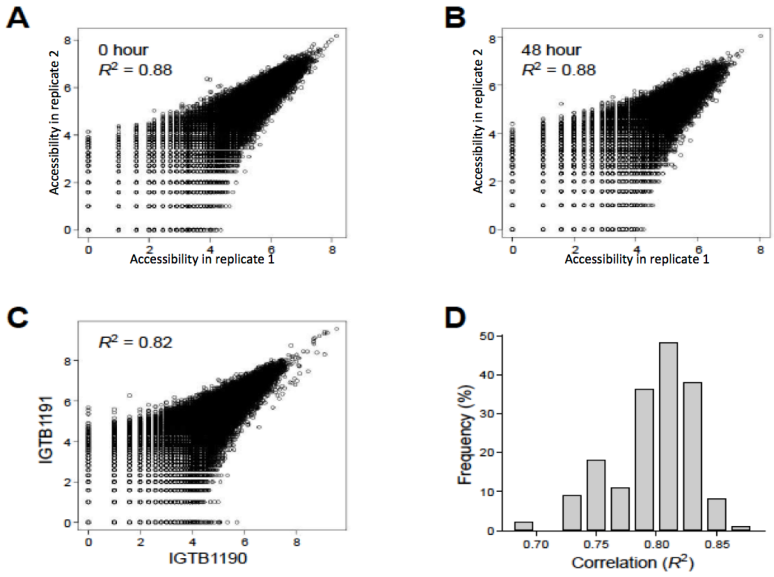

Supplementary Figure 2. ATAC-seq reproducibility. (**a**, **b**) Technical reproducibility. Scatter plots of chromatin accessibility (ATAC-seq signal, x and y-axes) for two replicate experiments of either unstimulated (a; 36,486 Th peaks) or activated (b; 52,154 Th_{stim} peaks) T cells. (**c**, **d**) Reproducibility between individuals. (c) Chromatin accessibility for activated T cells from individuals IGTB1191 (y-axis) and IGTB1190 (x-axis) (d) and histogram of correlations between every pairs of individuals for the 52,154 Th_{stim} peaks.

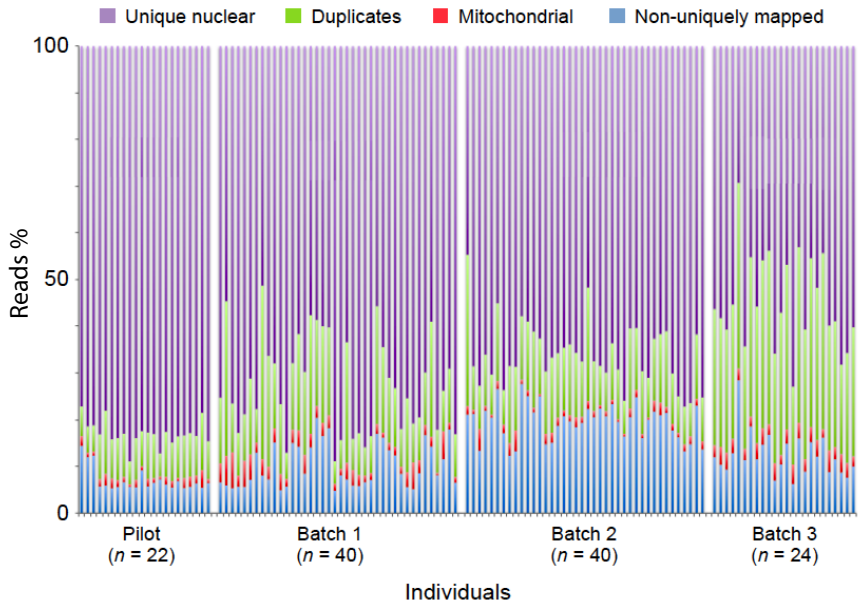

Supplementary Figure 3. ATAC-seq alignment rates. Each sample's (x-axis) percentage of reads (y-axis) that are non-uniquely mapped (blue), uniquely mitochondrial DNA (red), uniquely nuclear genomic duplicates (green), and uniquely nuclear genomic non-duplicates (purple).

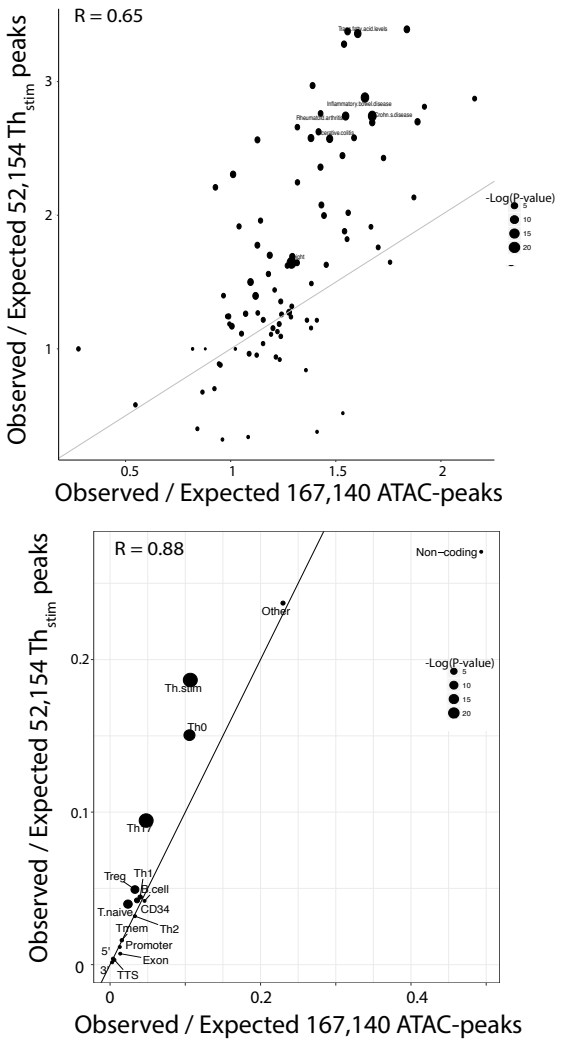

Supplementary Figure 4. Comparison of peak annotations in activated CD4$^+$ T cells. For each set of GWAS loci (a) or enhancer (H3k27Ac marks, b) features, shown is their observed over expected enrichment of proportions in 52,154 Th$_{stim}$ peaks called from pooling five individuals (y-axis; as in **Fig. 1**) or in 167,140 ATAC-peaks called from 105 individuals (x-axis, as in **Fig. 2**). Point size is scaled to associated significance (hypergeometric *P*-value).

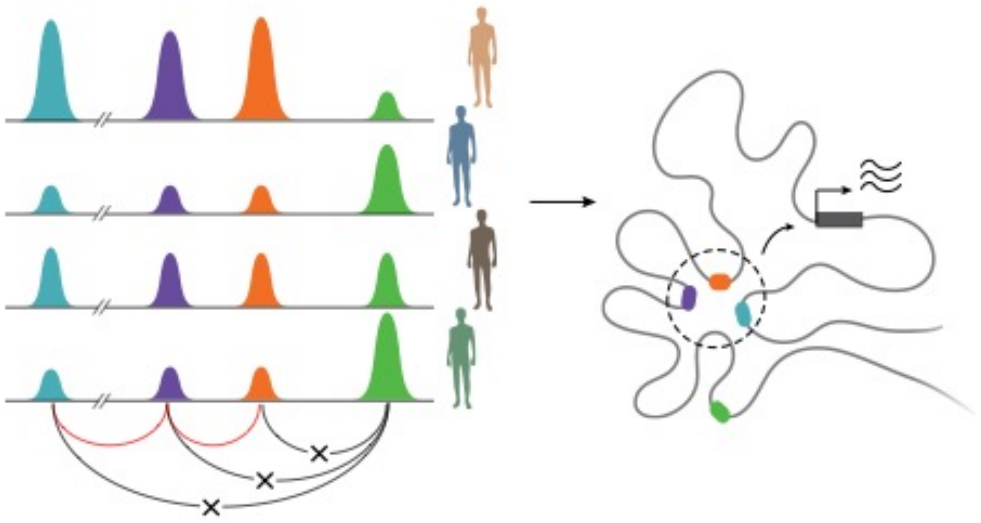

Supplementary Figure 5. Cartoon of co-accessible regions of accessible chromatin. Cartoon of the multiscale relationship between co-accessible regions across individuals and 3D genome structure.

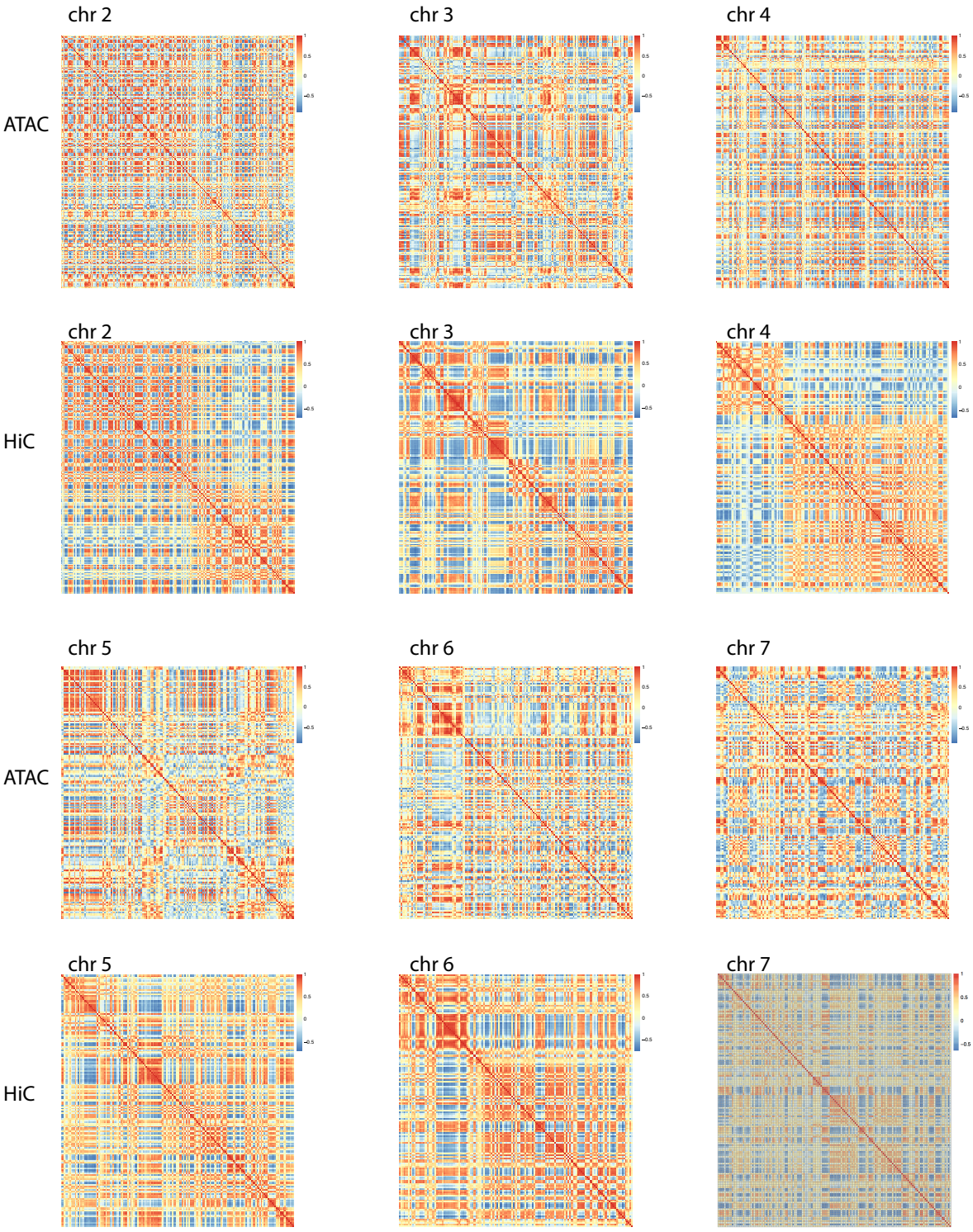
chr 2
chr 3
chr 4
ATAC
chr 2
chr 3
chr 4
HiC
chr 5
chr 6
chr 7
ATAC
chr 5
chr 6
chr 7
HiC

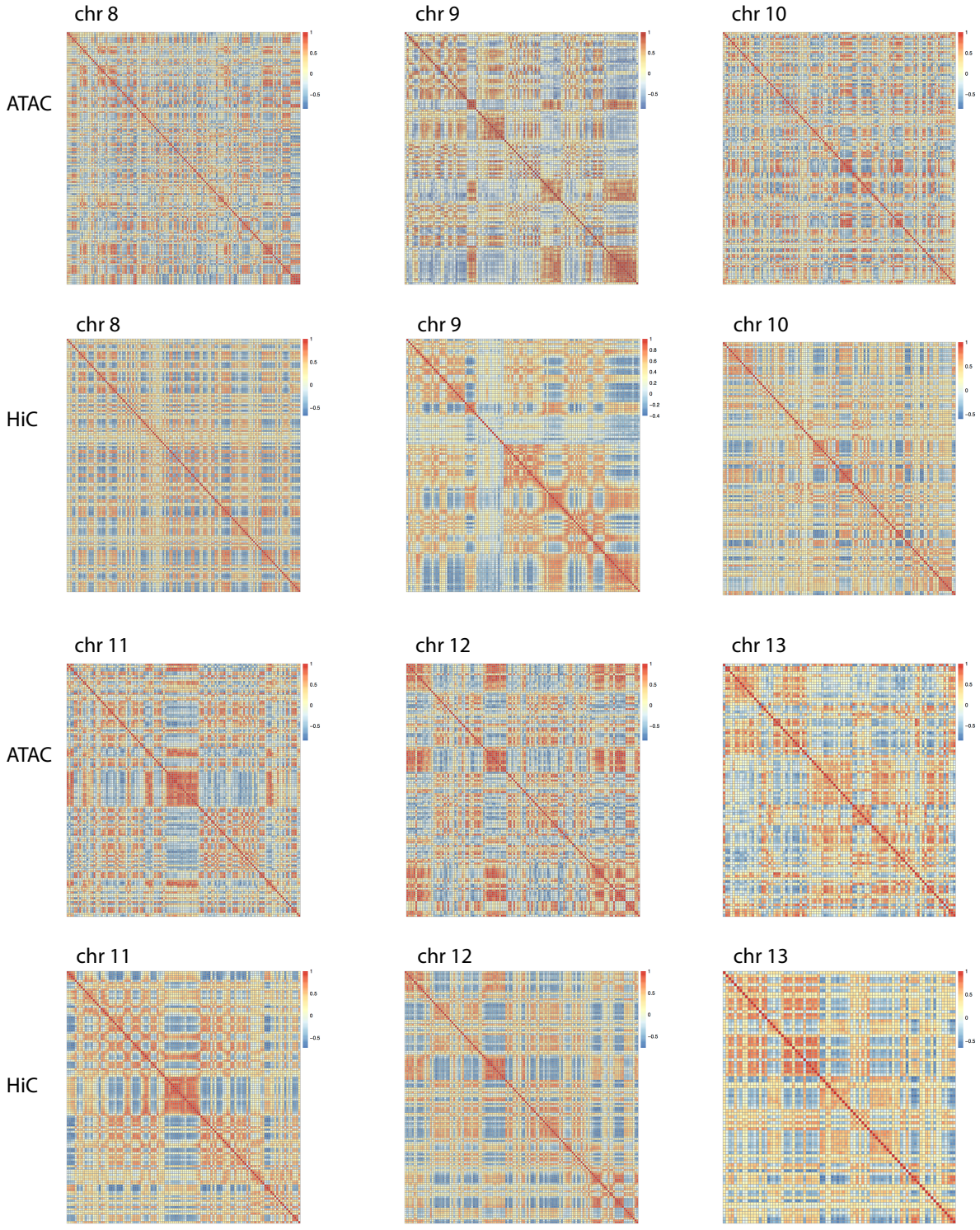
chr 8
chr 9
chr 10
ATAC
chr 8
chr 9
chr 10
HiC
chr 11
chr 12
chr 13
ATAC
chr 11
chr 12
chr 13
HiC


chr 14
chr 15
chr 16
ATAC
chr 14
chr 15
chr 16
HiC
chr 17
chr 18
chr 19
ATAC
chr 17
chr 18
chr 19
HiC

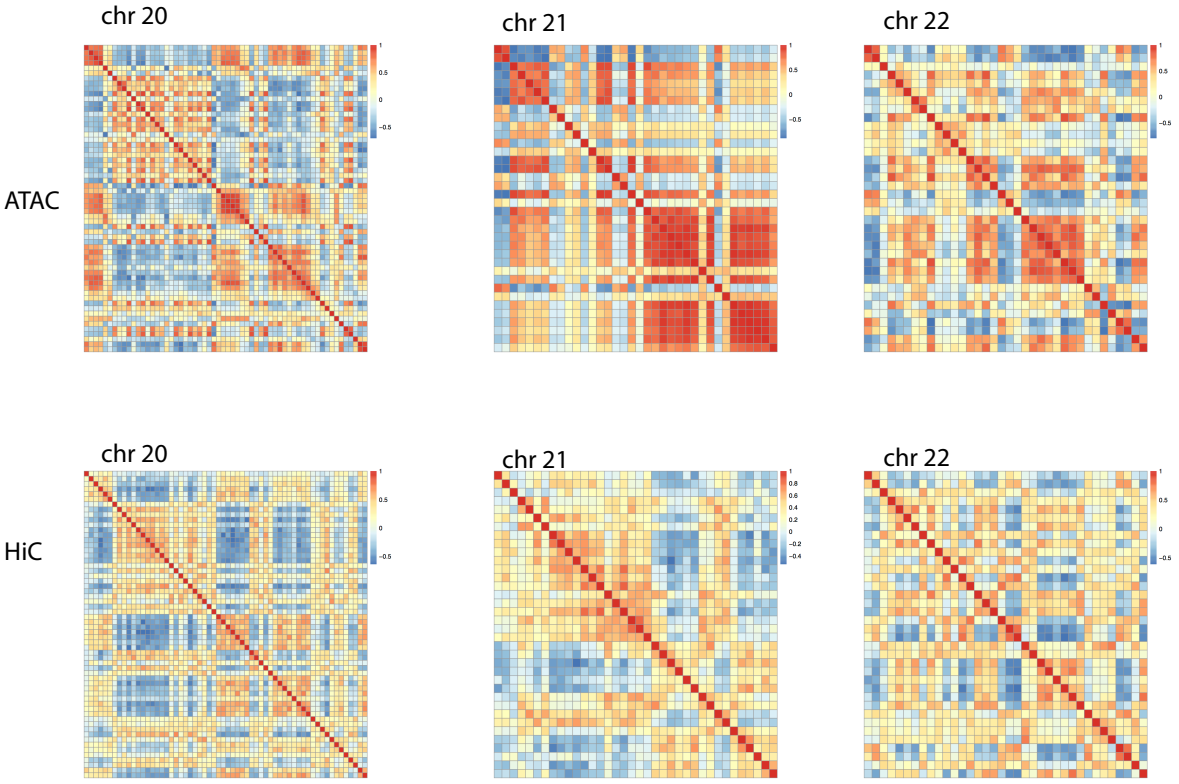

Supplementary Figure 6. Megabase scale inter-individual co-accessibility (by ATAC-peak) or physical interactions (by Hi-C). For each chromosome matching heat maps show the pairwise Pearson correlation in chromatin accessibility across 105 ATAC-seq profiles in ATAC-peaks binned into 1 Mb windows (top panel) and correlation of Hi-C interactions at 1 Mb resolution (bottom panel).

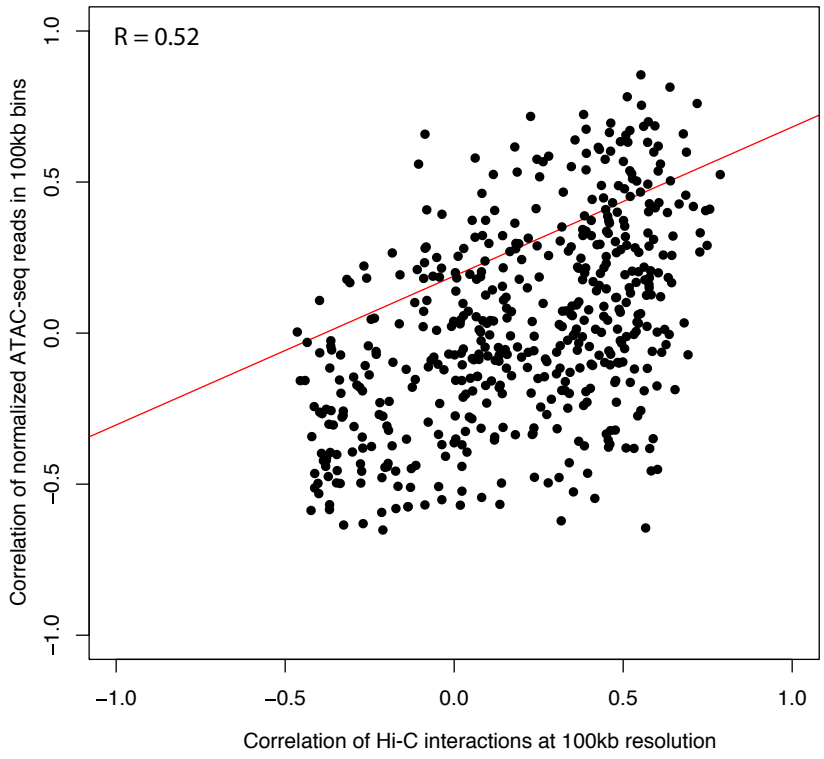

Supplementary Figure 7. Comparison of co-accessibility and Hi-C interactions.
For each pair of 100 kb windows (shown are 500 randomly sampled pairs) along chromosome 22 are the Hi-C interaction score (x-axis) and the correlation between ATAC-peaks (y-axis) (Pearson R = 0.52).

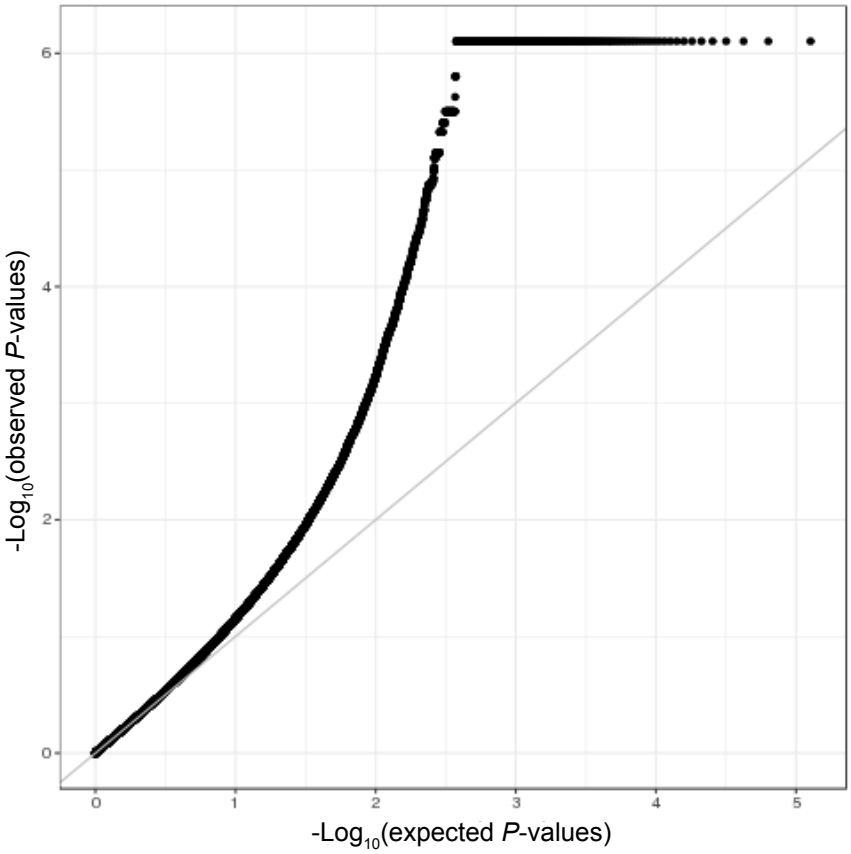

Supplementary Figure 8. Co-accessible peaks. Q-Q plot for all tests of correlation between co-accessible peaks within 1.5 Mb region around a target ATAC-peak.

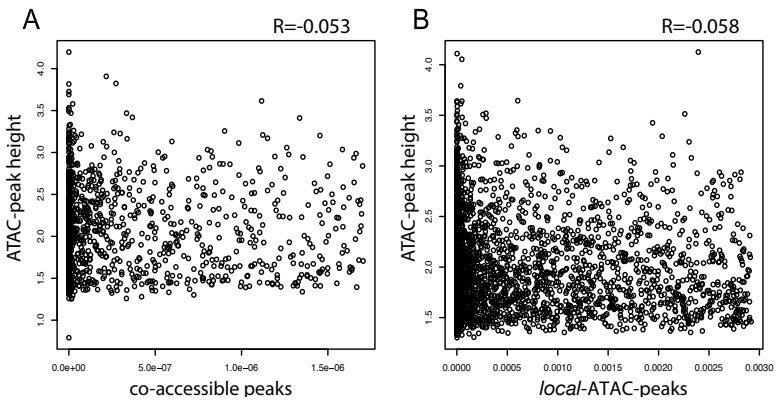

Supplementary Figure 9. Relation of ATAC-peak height and statistical significance of *local*-ATAC-peaks and co-accessible peaks. Relationship between ATAC-peak height (y-axis) and statistical significance (x-axis) of co-accessible peaks (a) and *local*-ATAC-peaks (b). Pearson R is marked on top, showing little relationship between the significance of local-association or co-accessibility and the strength of the peak.

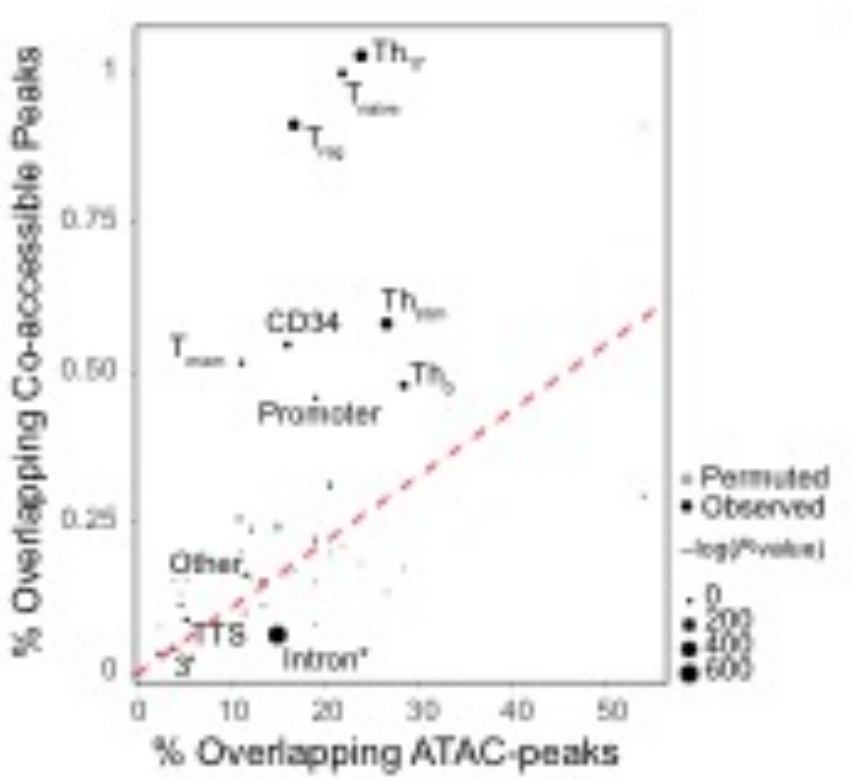

Supplementary Figure 10. Co-accessible peak overlap with Th cell enhancers. Percentages of enhancer annotations overlapping all ATAC-peaks (x-axis) *vs.* co-accessible peaks (y-axis). Real peaks (black) and permuted peaks (gray).

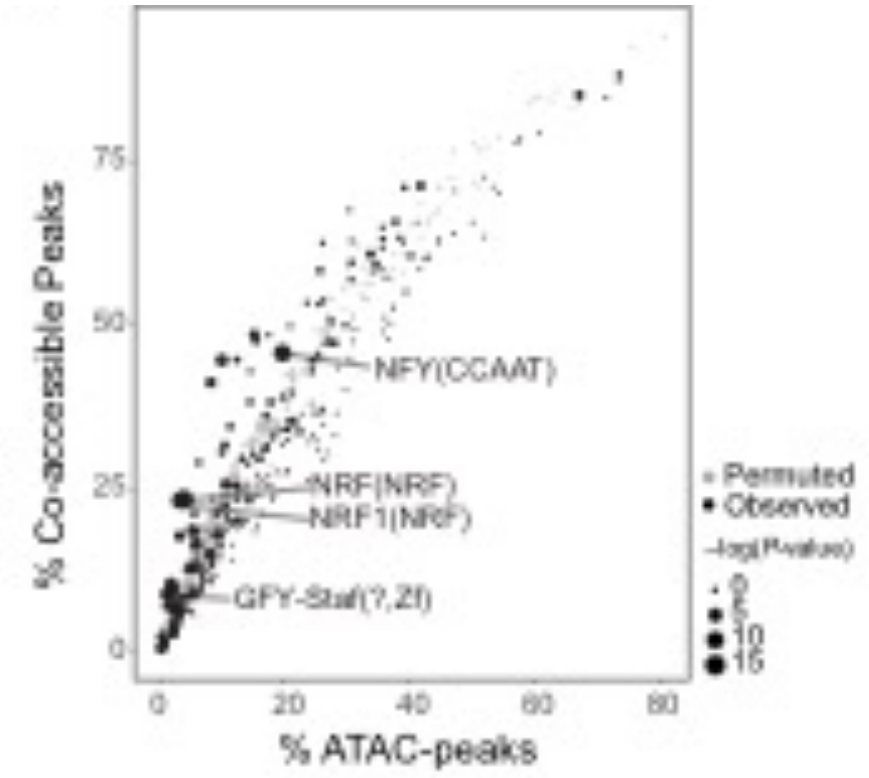

Supplementary Figure 11. Co-accessible peak TF motif enrichment. Percentage of ATAC-peaks (x-axis) *vs.* percentage of co-accessible peaks (y-axis) overlapping TF binding sites. Real peaks (black) and permuted peaks (gray).

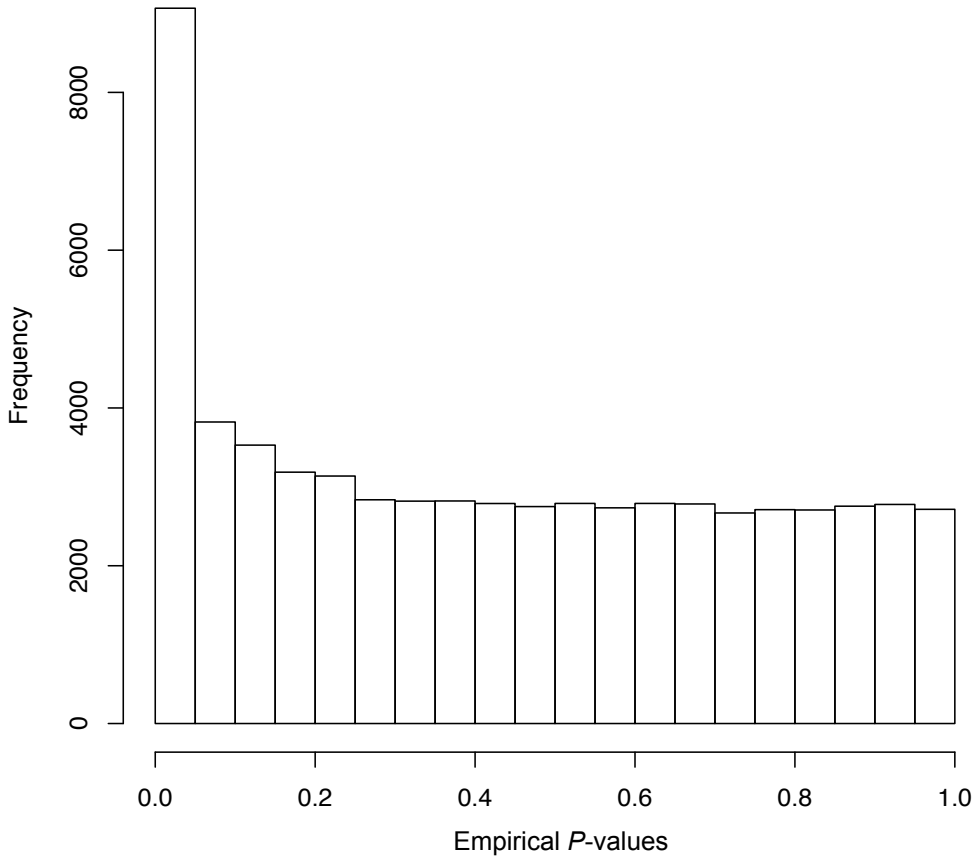

Supplementary Figure 12. *Local*-ATAC-QTL *P*-values. Distribution of the empirical *P*-values for the minimum statistical association per ATAC-peak containing a SNP.

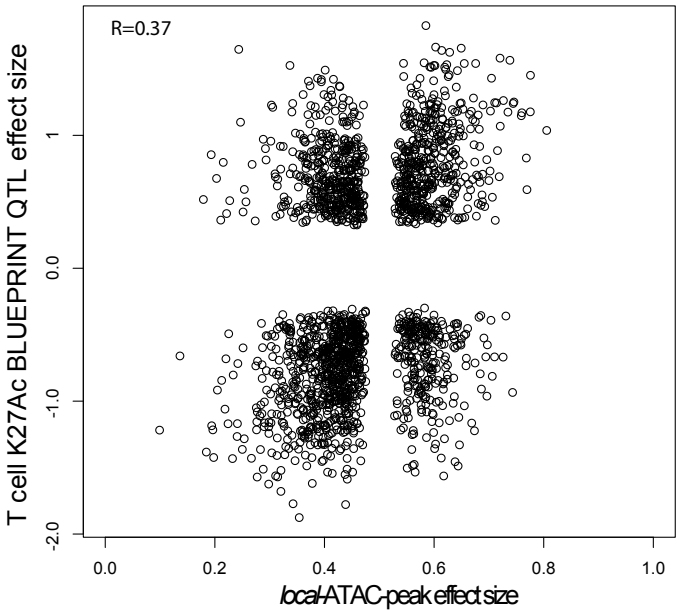

Supplementary Figure 13. Correlation to K27Ac QTLs identified in immune cells in the BLUEPRINT epigenome project. For each of 2,015 loci identified as both T cell K27Ac histone mark QTLs in the BLUEPRINT epigenome project (*1*) and as ATAC-QTLs in our analysis shown are their original effect sizes (y-axis) and the corresponding effect sizes by our *local*-ATAC-QTL analysis (x-axis).

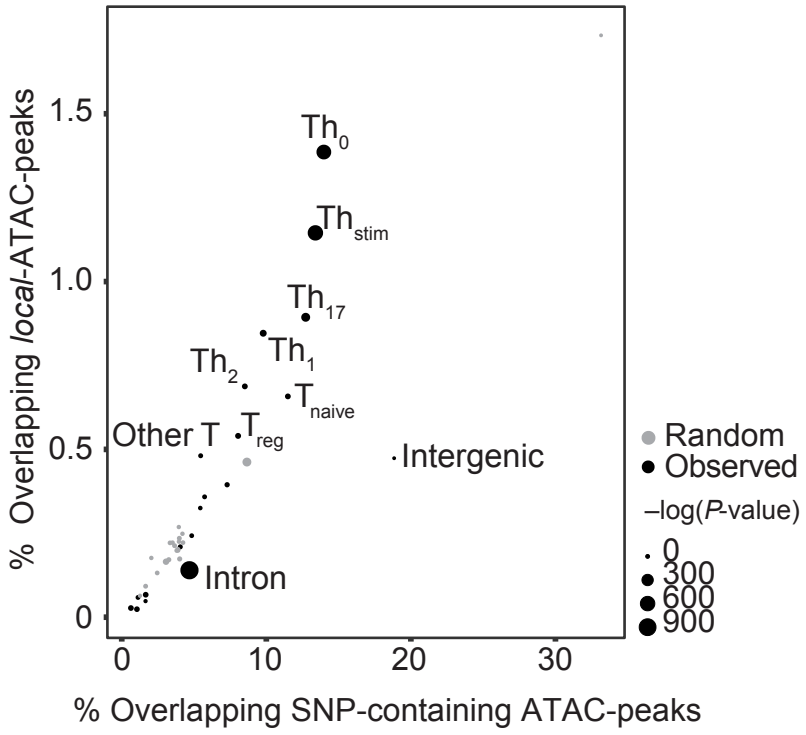

Supplementary Figure 14. Overlap of *local*-ATAC-peaks with T cell enhancers. Percentage of annotations overlapping SNP-containing ATAC-peaks (x-axis) *vs. local*-ATAC-peaks (y-axis). Real peaks (black) and permuted peaks (gray).

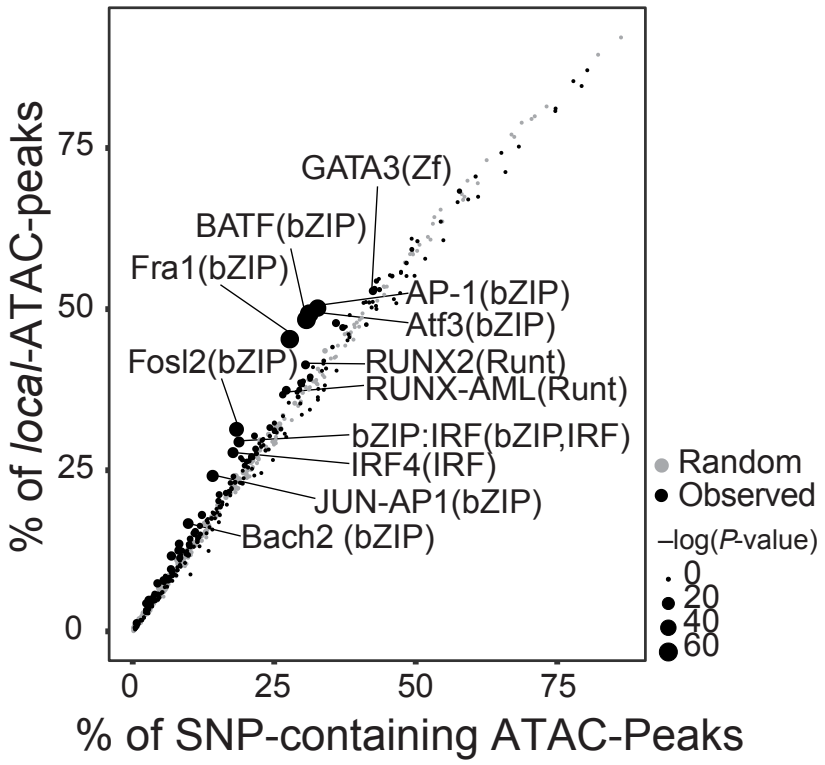

Supplementary Figure 15. TF motif enrichment of *local*-ATAC-peaks. Percentage of SNP-containing ATAC-peaks (x-axis) *vs.* percentage of *local*-ATAC-peaks (y-axis) overlapping each TF motif. Real peaks (black) and permuted peaks (gray).

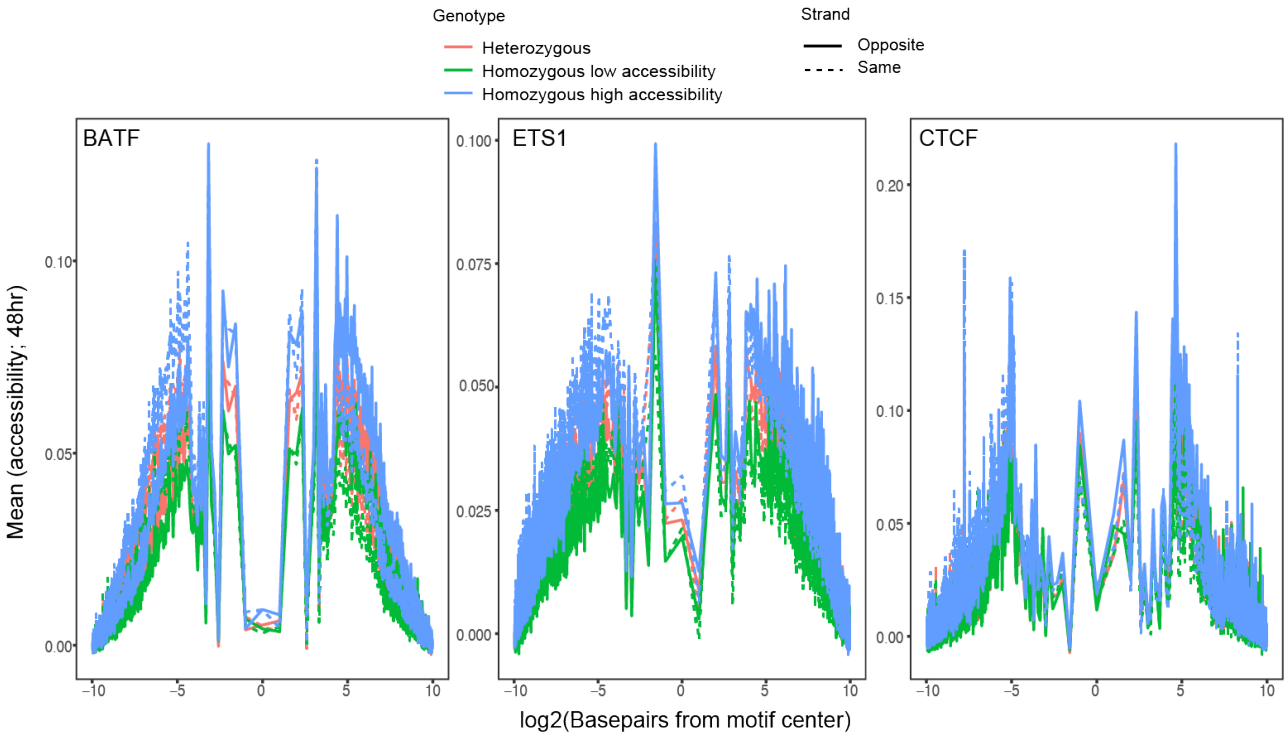

Supplementary Figure 16. Control for TF allele specific footprinting with *local*-ATAC-peaks. Aggregated chromatin accessibility (mean ATAC-seq signal, y-axis) in *local*-ATAC-peaks around BATF, ETS1, and CTCF binding sites previously identified by ChIP-seq (*2*) for the heterozygote (pink), homozygous with high ATAC-seq signal (blue) and homozygous with low ATAC-seq signal (green). Strand with the motif in dotted lines and the complementary strand with the motif in solid lines.

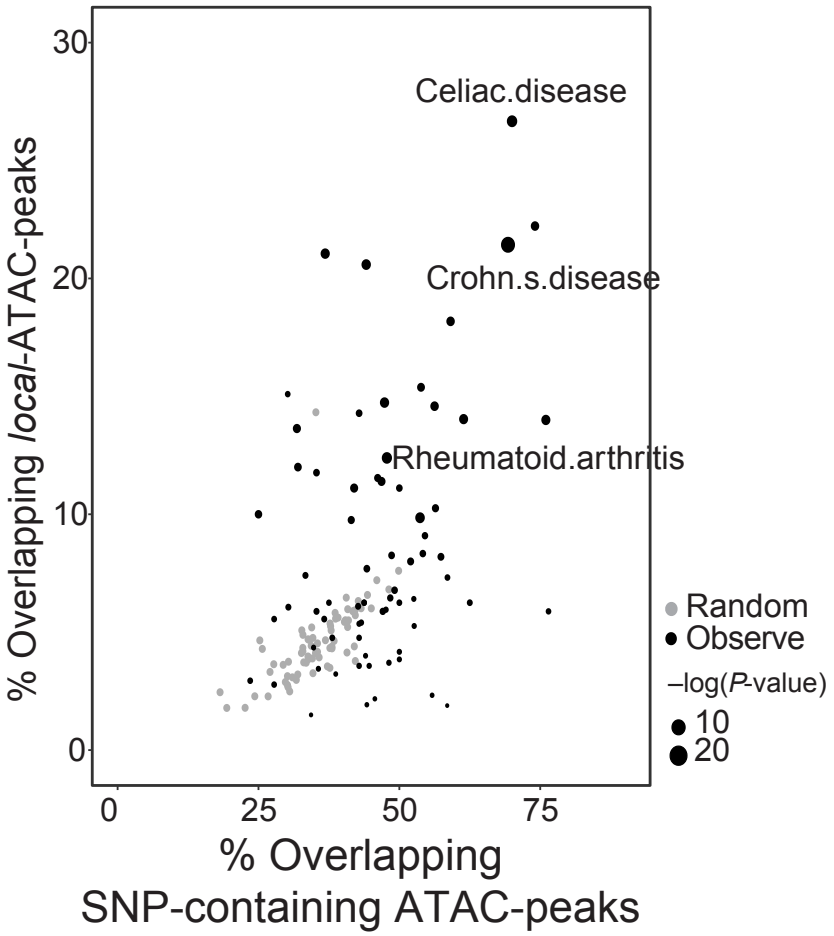

Supplementary Figure 17. Overlap of *local*-ATAC-peaks with GWAS loci. Percentages of GWAS loci overlapping with SNP-containing ATAC-peaks (x-axis) *vs. local*-ATAC-peaks (y-axis). Real peaks (black) and permuted peaks (gray).

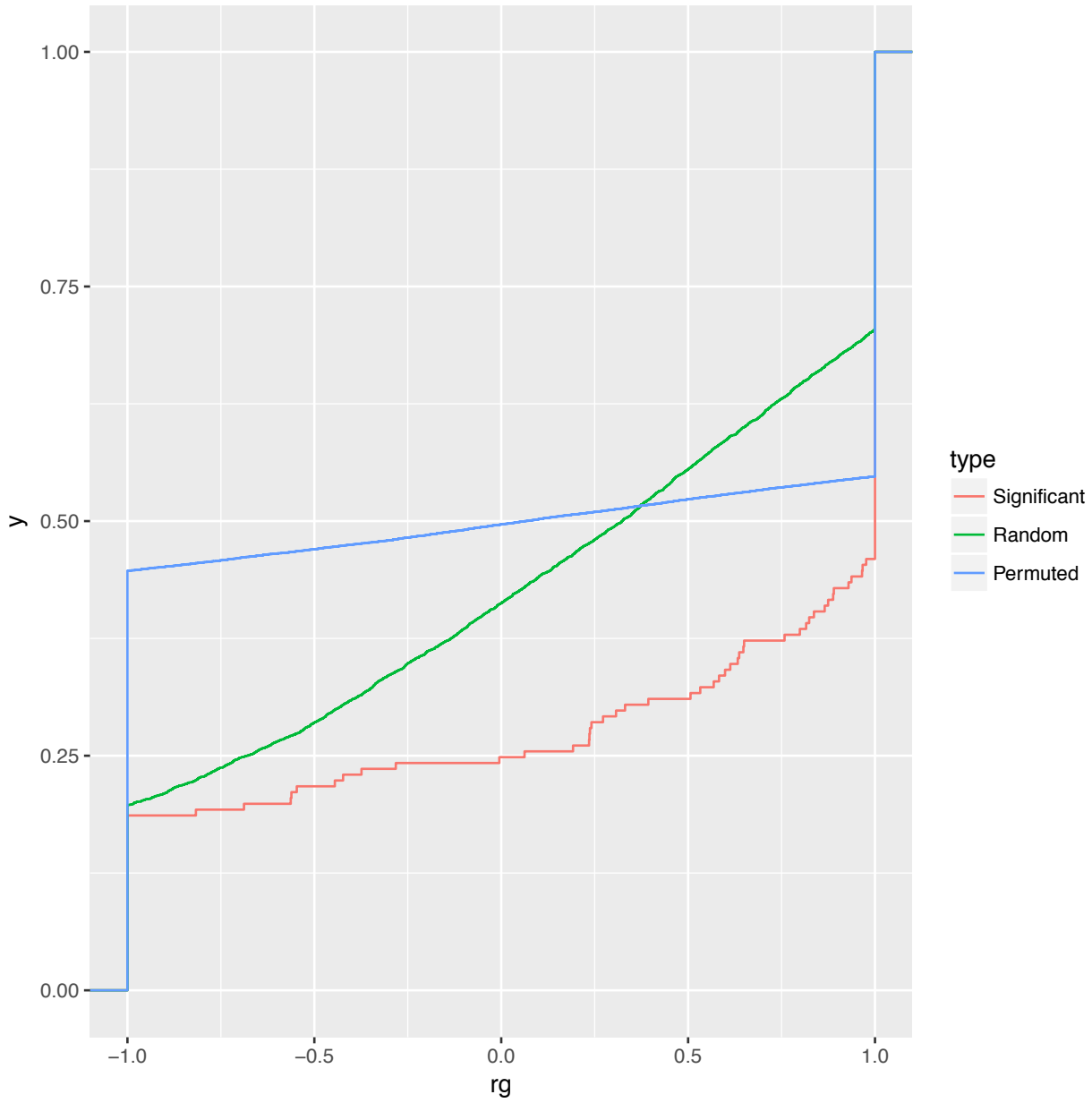

Supplementary Figure 18. Cumulative Distribution Function of genetic correlation. Colored by significant (red), randomly sampled (green) or permuted (blue) pairs of *local*-ATAC-peaks.

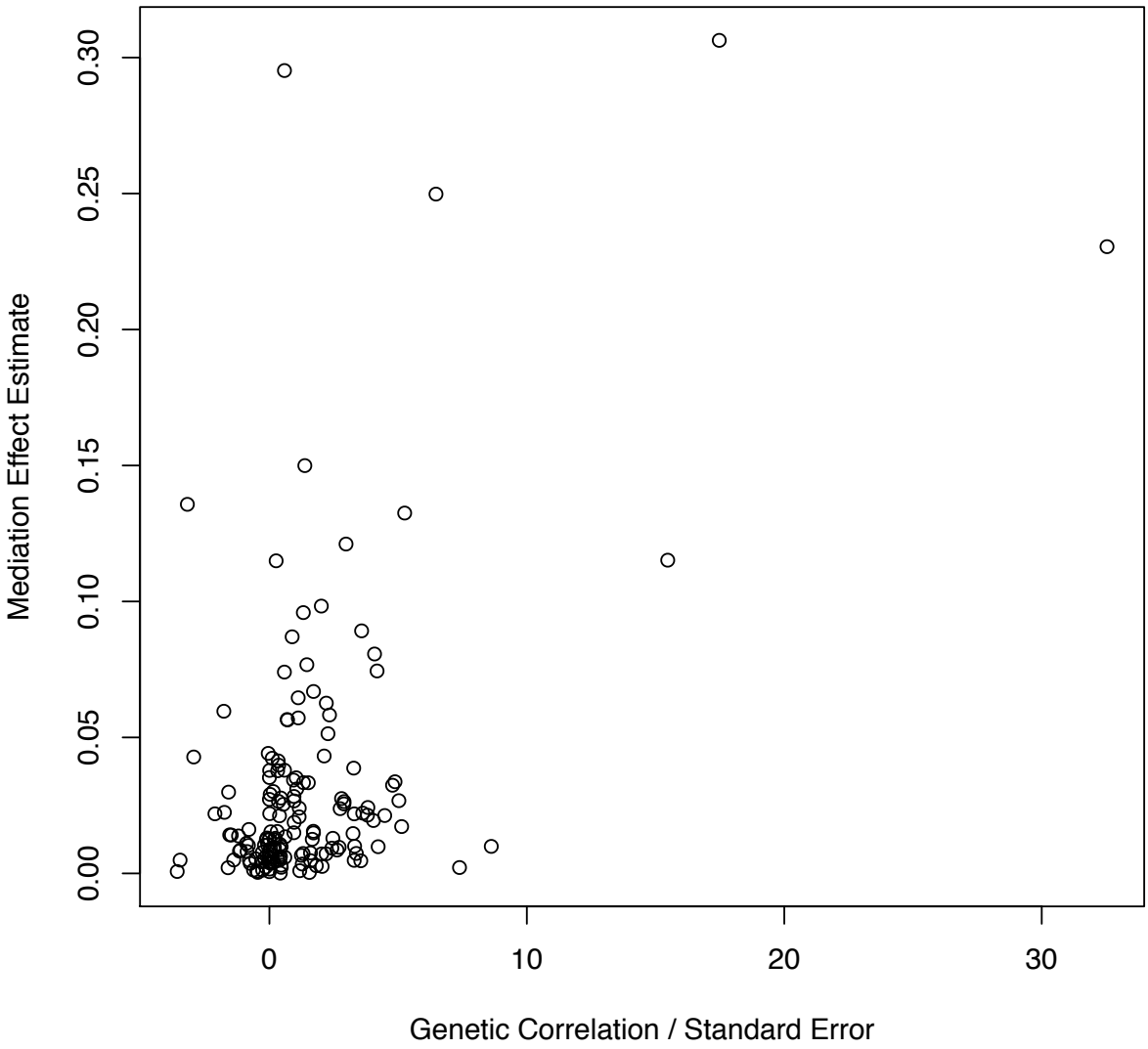

Supplementary Figure 19. Genetic correlation *vs.* Mediation Effect Estimate. Genetic correlation (weighted by the standard error) (x-axis) *vs.* the mediation effect estimate (y-axis) for 161 pairs of *local*-ATAC-peaks and eGenes that converged.

References:

1. L. Chen *et al.*, Genetic Drivers of Epigenetic and Transcriptional Variation in Human Immune Cells. *Cell* **167**, 1398-1414 e1324 (2016).
2. P. Kheradpour, M. Kellis, Systematic discovery and characterization of regulatory motifs in ENCODE TF binding experiments. *Nucleic Acids Res* **42**, 2976-2987 (2014).